Evaluation of a Method for Estimating Configuration Parameters in Bistatic Radars Using Directive Antennas

Xavier Neyt*, Fabian D. Lapierre†**, Jacques G. Verly†
*Royal Military Academy, Electrical Engineering Department,
Avenue de la Renaissance, 30, B-1000, Bruxelles, Belgium
†University of Liège, Department of Electrical Engineering and Computer Science,
Sart-Tilman, Building B28, B-4000, Liège, Belgium
Xavier.Neyt@elec.rma.ac.be, {F.Lapierre; Jacques.Verly}@ulg.ac.be

Abstract: The method proposed in this paper aims at performing an automatic estimation of the clutter power spectrum (PS) locus in order to perform an optimum range-dependence compensation to finally provide an estimate of the snapshot covariance matrix. The method is shown to estimate reliably the clutter PS locus even for complex bistatic scenarios involving directional antenna patterns. Performance of the method is analyzed, first with respect to the required sample-support size and then in comparison to other methods.

Keywords: Radar, bistatic, STAP, range-dependence, non-stationarity

1. Introduction

Mitigation of radar ground clutter via STAP requires the estimation of the interference-plus-noise (I+N) snapshot covariance matrix (CM) at each range. The typical approach is to average single-realization sample CM at neighboring ranges. However, in most configurations, snapshots have range-dependent spectral characteristics leading to a poor estimate of the CM at the considered range.

Among methods proposed to perform the range-dependence compensation, the method described in [1] is able to perform an exact range compensation for any range and for any monostatic (MS) or bistatic (BS) configuration. This method is based on the registration, prior to averaging, of the clutter PS at neighboring ranges to that at the range of interest. However, this method relies on the knowledge of the configuration parameters, i.e., receiver location relative to the transmitter (R_{TR}, θ, ϕ) and velocity orientation α_R of the receiver R with respect to the velocity orientation of the transmitter T, velocities v_R of R and v_T of T and receiver antenna orientation δ. Even if this method allows for the estimation of the configuration parameters, the estimation algorithm is only intended for use with omnidirectional sensors.

The proposed method aims at estimating the clutter PS locus, hence indirectly providing an estimate of the configuration parameters, from the single-realization snapshots at different ranges either for omnidirectional or for directional antenna patterns.

In Section 2, the definition and properties of the clutter PS are reviewed. In Section 3, the parameter estimation method is detailed. The performance of this estimation method is discussed in Section 4. The performance is discussed both in terms of PS locus estimation accuracy and in terms of end-to-end performance using the SINR loss.

2. Clutter PS locus

The clutter echo at any particular range is, by definition, the echo backscattered from scatterers located on the related isorange curve. Since each scatterer on the isorange can be represented by a point in the spatial-frequency (ν_s)-Doppler-frequency (ν_d) space, the spectrum of the theoretical CM of the clutter snapshot at some range has the shape of a ridge, called the clutter ridge.

The parametric equations of the clutter PS locus are obtained by finding expressions for the values of ν_d and ν_s along the considered isorange curve. Figure 1 compares the clutter PS to the clutter PS locus. Since the clutter PS locus perfectly characterizes the location of the clutter PS, we will use the former representation to further analyze the behavior of the ground clutter.

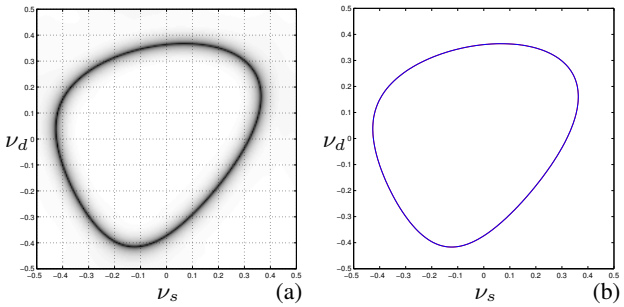

Fig. 1. Correspondence between (a) the clutter PS and (b) its geometric locus for a particular BS scenario and range.

Furthermore, with the exception of the MS sidelooking configuration (and some particular BS configurations), the shape of the clutter PS locus varies with the BS range [1], [2]. By stacking clutter PS loci corresponding to increasing BS ranges, one obtains a surface that helps un-

**Research Fellow of the Belgian National Fund for Scientific Research.

derstand the estimation method. This surface is illustrated in Fig. 2 for two different BS scenarios.

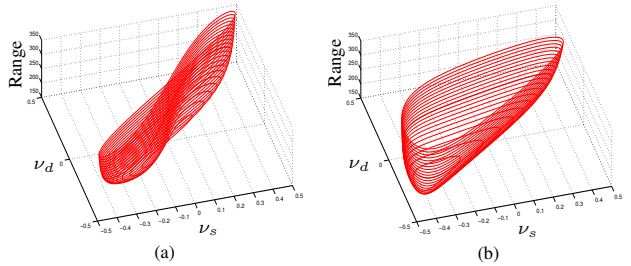

Fig. 2. Clutter PS locus surfaces for two selected BS scenarios.

The antenna pattern modulates the amplitude A of the echo received from each scatterer S, i.e.,

$$A(s) = \sigma\, k(R) G_\theta^T(\theta_T) G_\phi^T(\phi_T) G_\theta^R(\theta_R) G_\phi^R(\phi_R), \qquad (1)$$

where s is the location of S, σ is the radar cross section, $k(R)$ is a constant depending on the BS range R, $(\theta_T,\ \phi_T)$ and $(\theta_R,\ \phi_R)$ are the antenna elevation and azimuth angles under which S is seen by the transmitting antenna and by the receiving antenna, respectively. G_θ^T and G_ϕ^T are the transmitter antenna pattern in elevation and azimuth, respectively. Similarly, G_θ^R and G_ϕ^R are the receiver elevation and azimuth antenna patterns. Since every S can be located in the (ν_s, ν_d)-plane, the antenna patterns directly affects the amplitude of the clutter PS as shown in Fig. 3 for two BS scenarios where a directive transmit antenna pattern is considered.

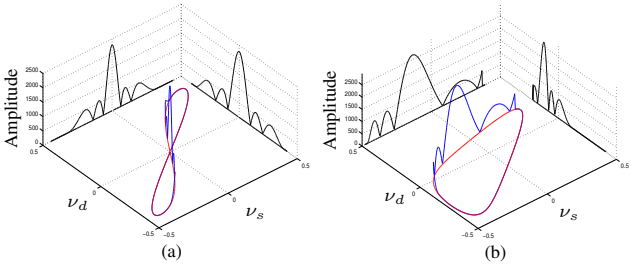

Fig. 3. Clutter PS amplitude for two selected BS configurations.

3. Parameter estimation method

The method exploits the fact that the PS of individual realizations of snapshots exhibit peaks located along the clutter PS locus. By extracting the location of these peaks and fitting the mathematical model of the clutter PS locus, the parameters of the model can be estimated.

The starting point of the method is a set of snapshot realizations obtained at different ranges. Each snapshot is assumed to be composed solely of ground clutter and noise. The contributing scatterers are located on the isorange curve under consideration and the backscattered signal is assumed to have a random phase with uniform distribution. The snapshot consists in one realization of this random process. Since the contributing scatterers are located on one isorange curve, the snapshot PS will be concentrated along the clutter PS locus. This is illustrated in Fig. 4. The subfigures differ in two ways. Each correspond to a different type of antenna pattern and to a different realization of the underlying random process. This last fact explains why the peaks fall in different places. In each case, the (theoretical) clutter PS locus is also shown. Each snapshot PS exhibits peaks located along

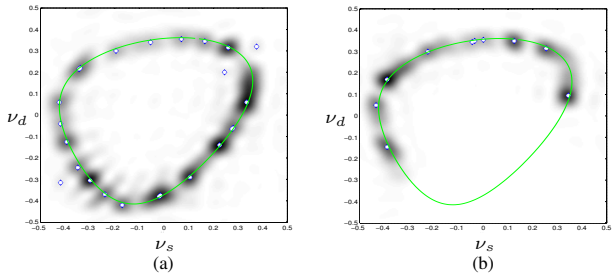

Fig. 4. PS of two snapshots, with (a) a uniform antenna pattern and (b) with a directive antenna pattern.

the clutter PS locus. Since the actual snapshot size is very small, the Fourier spectral estimation is very smooth and the extraction of these peaks can be performed by a local maximum extraction as indicated by the white dots in Fig. 4. To remove the spurious peaks that appear, a thresholding operation on the amplitude of the peaks is performed.

The next step of the method is to fit the mathematical clutter PS locus model to the location of the extracted peaks. Since this model is designed to be applied to all ranges, the model fitting provides more accurate results if the locations of the peaks at all ranges are used. This can be interpreted as fitting a 3D clutter PS locus (surface) to the cloud of extracted peaks.

The quality of the fit is measured by a cost function. This cost function is taken as the sum of the euclidean distances of the peaks to the closest points on the clutter PS locus model at the same range.

To discard spurious peaks, the contribution of each peak to the global cost function is weighted by the relative amplitude of the peak. Furthermore, peaks located at a distance from the model larger than a certain threshold are weighted with a weight equal to zero and hence do not contribute to the cost function.

The cost function is minimized using a variation of the simplex algorithm. This method offers the advantage that the derivative of the cost function with respect to the parameters does not need to be computed. As is to be expected, the cost function is non quadratic and local minima exist. These local minima correspond to a natural symmetry of the model.

Figure 5 shows a 2D cut in the 6D cost function hypercube (for a particular BS scenario) along the plane of the parameters (R_{TR}, δ). The true parameter values are indicated by a white dot, approximately in the center of the figure. Local minima at $R_{TR} = 0$ are clearly visible. The 3D clutter PS locus obtained when convergence to a local minima is reached is illustrated in Fig. 6(a). The 3D clutter PS locus obtained at the global minimum is illustrated in Fig. 6(b). Clearly, the latter best fits the extracted peaks (indicated by +'s).

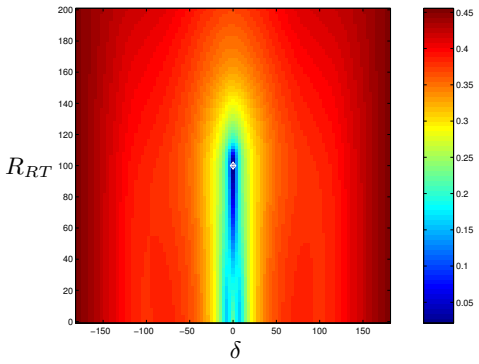

Fig. 5. 2D slice in the 6D cost function hypercube. The slice shown is the (R_{TR}, δ) plane.

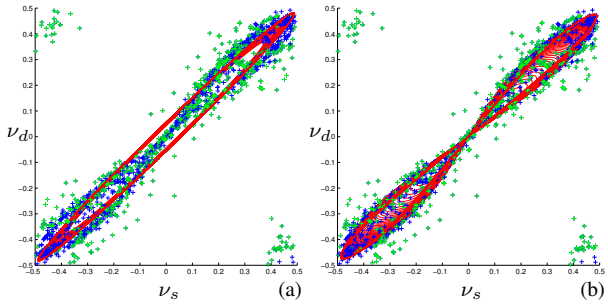

Fig. 6. Estimated 3D clutter PS locus (solid lines) and extracted peaks (+'s) when converging (a) to a local minima and (b) to the global minimum.

In order to avoid getting trapped in local minima, several initial conditions have to be considered. These initial conditions are obtained by performing a guided minimization taking into account the physics of the problem. Different guided minimizations are considered and the parameter set yielding the smallest cost-function value is retained.

One of these guided minimization takes into account the fact that, at long BS ranges, the behavior of the clutter PS locus tends to be close to that of an MS configuration. Hence the receiver position parameters (R_{TR}, θ, ϕ) have little influence on the clutter PS locus for long BS ranges. Therefore, the angular parameters (α_R, δ) and the transmitter velocity v_T will be estimated using the peaks extracted from snapshots at long BS ranges only. Note that v_R is logically assumed to be known.

Once a first estimate of (α_R, δ, v_T) is obtained, the parameters (R_{TR}, θ, ϕ) are estimated using the snapshots corresponding to short BS ranges. The clutter PS locus actually varies most for short ranges. Hence, in order to maximize the sensitivity of the cost function to the parameters (R_{TR}, θ, ϕ) and to avoid the dominance of the snapshots at long ranges, only the snapshots corresponding to the shortest ranges are used.

Once a reasonable initial estimate is obtained, a global minimum search is performed, resulting in the simultaneous estimation of all the parameters.

More details about this method and the other guided minimizations examined can be found in [3].

4. Results

In this section, the performance of the parameter estimation method are first evaluated in terms of accuracy of the clutter PS locus estimation. The metric used to this end is the RMS distance between the estimated 3D clutter PS locus and the true 3D clutter PS locus. The influence of the spectral resolution and of the number of snapshots on the estimation accuracy is also evaluated.

Subsequently, the end-to-end performance of the parameter estimation method combined with a variant of the range-dependence compensation method proposed in [1] is reported.

4.1. Parameter estimation performance

Figure 7 represents cuts in the clutter PS locus surface showing the true clutter PS locus and the estimated clutter PS locus. In the case of omnidirectional antenna patterns (Fig. 7 (a)), a very satisfying fit is obtained. In the case of directional antenna patterns (Fig. 7 (b)), only part of the clutter PS is available for the estimation as a result of the fact that only part of the isorange curve is illuminated. Therefore, only part of the clutter PS can be fitted. The corresponding parameters may not correspond to physical reality, but this is irrelevant. Indeed, there is no clutter energy where the clutter PS locus did not fit.

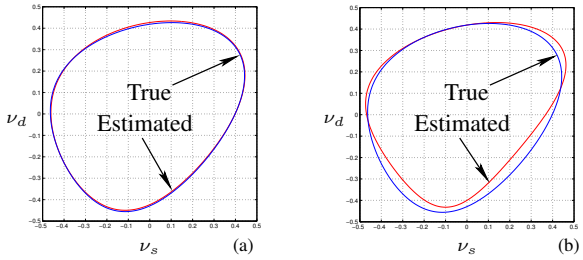

Fig. 7. True clutter PS locus and estimated clutter PS locus. (a) omnidirectional antenna pattern, (b) directional antenna pattern.

4.2. Performance estimation as a function of the spectral resolution

The parameter estimation method consists in fitting a mathematical model to the peaks extracted from the PS of the measured snapshots. Since the spectral estimation used is quantized in angle-Doppler, the location accuracy of these peaks directly depends on the resolution of the spectral estimator used to compute the PS of the snapshots. The concept of resolution here is to be understood as the number of samples (along both frequency axes) at which the PS is evaluated. The larger the number of available samples is, the smaller the location quantization error will be and the more accurate the location of the peaks will be. On the other hand, the higher the number of required samples is, the higher the computational requirements will be. The computational requirements typically increase as $(N \log N)^2$, where N is the number of samples considered.

Figure 8 shows the evolution of the value of the RMS error

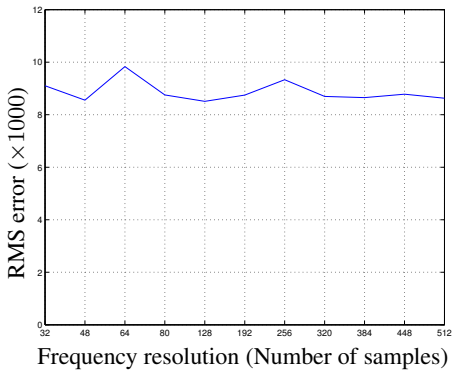

Fig. 8. Evolution of the RMS error between the estimated 3D clutter PS locus and the true 3D clutter PS locus as a function of the resolution of the PS, expressed in number of samples.

between the estimated 3D clutter PS locus and the true 3D clutter PS locus as a function of the spectral resolution.

As can be seen, the RMS error is essentially unaffected by the quantization of the peak locations. Actually, a decrease of the location accuracy of the peaks can be modeled as causing a random jitter of the peak locations, both in angle and in Doppler coordinates. On the other hand, some particular pulse-to-pulse and element-to-element signal decorrelation [4] such as ICM also causes a jitter in the angle-Doppler location of the peaks. In [5], the proposed method was shown to be also essentially insensitive to ICM. The reason was that, as long as the distribution of the location jitter is symmetric around the true (mean) location value, the RMS distance between the peaks and the model is minimum when the model is at the mean location of the peaks. The same explanation holds here since quantization jitter is usually considered as uniformly distributed.

4.3. Performance estimation on a reduced dataset

The required computational complexity is proportional to the number of peaks considered in the fitting algorithm. Obviously, reducing the number of snapshots reduces the number of peaks. Performance of the estimation algorithm was investigated when using a reduced number of snapshots to compute the estimate. Figure 10 shows the RMS distance between the estimated clutter PS locus and the true clutter PS locus as a function of two parameters. The parameter Δk is the range interval over which the estimation is performed and N_k is the number of snapshots considered within that range interval. These two parameters are illustrated in Fig. 9. In the best case, $N_k = \Delta k$, i.e., all the available snapshots are used to compute an estimate of the parameters. A smaller sample-support implies that $N_k < \Delta k$, i.e., that some snapshots are not used in the parameter estimation. If $N_k < \Delta k$, the N_k snapshots considered are evenly spaced in range (among the Δk available snapshots). Obviously, the larger Δk, the more snapshots will potentially be available to perform the estimation. This explains the lower-triangular shape of the graph in Fig. 10.

As can be seen, performance is very stable, even when a very small number of snapshots is used. However, performance degrades when Δk is large and N_k is low (only a few snapshots are used). The reason for this degradation lies in the fact that there is insufficient information to make the estimation converge to the true configuration parameters.

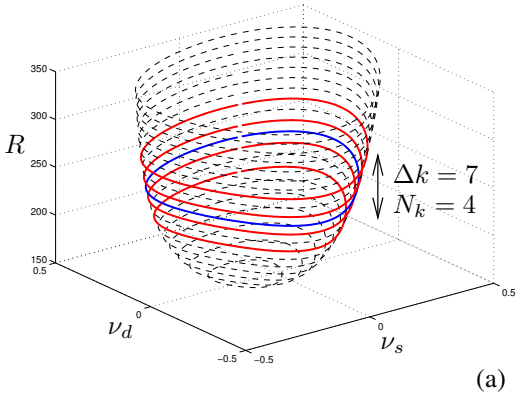

Fig. 9. Illustration of the parameters used when evaluating the sample-support requirements.

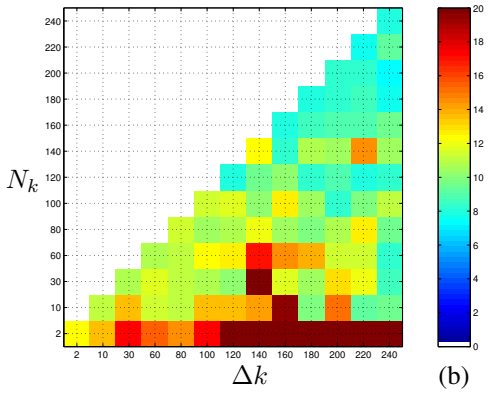

Fig. 10. Graph of cost function as a function of the number of snapshots N_k used to perform the parameter estimation and of the range interval Δk.

4.4. End-to-end performance

Figure 11 shows the PS of the I+N CM estimated using two different methods in the case of omnidirectional antenna patterns. The CM estimate whose PS is depicted in Fig. 11(a) was obtained using the sample CM. As can clearly be seen, this estimate "leaks" energy outside the true clutter PS locus, depicted as a thin line on the graph. This is due to the range dependence of the PS of the clutter snapshots. On the other hand, the CM estimate whose PS is depicted in Fig. 11(b) was obtained using a variant of the range-dependence compensation method proposed in [1] combined with the configuration-parameter estimation method proposed in this paper. Clearly, the PS of the latter estimate closely follows the true clutter PS locus.

The parameter estimation method described here was embedded in the so-called "Estimated Parameters (EP) range-dependence compensation" method proposed in [1]. This allows us to test our method end-to-end. Figure 12 shows the SINR loss obtained using the proposed method (EP). For comparison, the performance of the optimum processor (OP) and that of the straight-averaging processor (SAP) are also

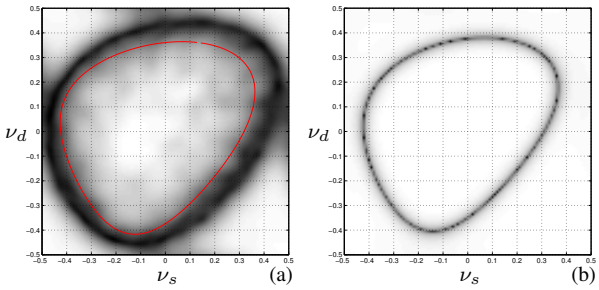

Fig. 11. PS of the estimated I+N covariance matrix (a) using the sample CM and (b) using the proposed method, for the case where antennas with omnidirectional patterns are used.

shown. The performance of the proposed method is very close to that of the OP. Due to the range-dependence of the clutter PS, the SAP causes undernulling of the clutter.

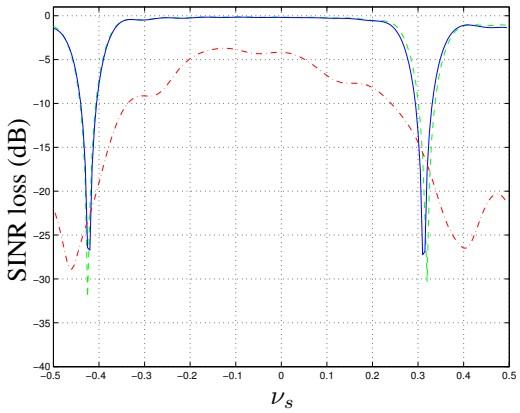

Fig. 12. Cuts of SINR loss at $\nu_d = 0.2$ for the OP (dashed curve), SAP (bottommost, dash-dotted curve) and EP (solid curve) when the antennas have omnidirectional patterns.

Figure 13 shows the PS of the I+N CM estimated using two different methods in the case of directional transmit antenna patterns. The CM estimate whose PS is depicted in Fig. 13(a) was obtained using the sample CM. As can clearly be seen, this estimate "leaks" energy outside the true clutter PS locus, depicted as a thin line on the graph. This is due to the range-dependence of the PS of the clutter snapshots. On the other hand, the CM estimate whose PS is depicted in Fig. 13(b) was obtained using a variant of the range-dependence compensation method proposed in [1] combined with the configuration-parameter estimation method proposed in this paper. Clearly, the PS of the latter estimate closely follows the true clutter PS locus.

Figure 14 shows the SINR loss obtained when a directional transmit antenna pattern is used. The performance of the proposed method is again nearly indistinguishable from that of the OP.

5. Conclusions

A new method for estimating the bistatic radar configuration parameters is proposed. The method is shown to be able to estimate the clutter power spectrum locus both when omnidirectional and directional antennas are considered. The

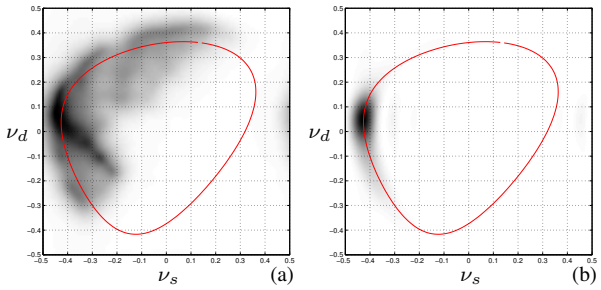

Fig. 13. PS of the estimated I+N covariance matrix (a) using the sample CM and (b) using the proposed method, for the case where a transmit antenna with a directional pattern is used.

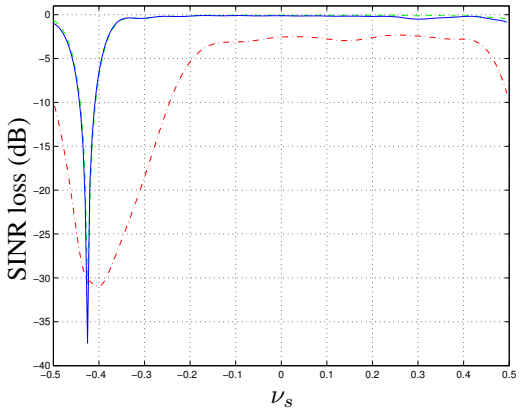

Fig. 14. Cuts of SINR loss at $\nu_d = 0.2$ for the OP (dashed curve), SAP (bottommost, dash-dotted curve) and EP (solid curve) when the transmit antenna has a directional pattern.

method proposed was also shown to have acceptable performance when considering tradeoffs aiming at reducing the processing requirements. In particular, reducing the PS resolution does not lead to measurable performance degradation. Furthermore, in order to maintain reasonable performance when reducing the sample-support, the range span over which the estimation is performed should be kept as large as possible.

The method proposed in this paper is to be integrated with a range-dependence compensation method in order to estimate the interference+noise covariance matrix. The end-to-end performance of the combination of these two methods is shown to be very close to that of the optimum processor, which uses the true interference+noise covariance matrix.

References

[1] F. D. Lapierre and J. G. Verly, "Registration-based solutions to the range-dependence problem in STAP radars," in *Adaptive Sensor Array Processing (ASAP) Workshop*, MIT Lincoln Laboratory, Lexington, MA, Mar. 2003.

[2] Y. Zhang and B. Himed, "Effects of geometry on clutter characteristics of bistatic radars," *IEEE National Radar Conference, Huntsville*, pp. 417–424, 5-8 May 2003.

[3] X. Neyt, F. D. Lapierre, and J. G. Verly, "Principle and evaluation of a registration-based range-dependence compensation method for STAP in case of arbitrary antenna patterns and simulated snapshots," in *Proc. Adaptive Sensor Array Processing Workshop*, MIT Lincoln Laboratory, Lexington, MA, Mar. 2004.

[4] J. R. Guerci, "Theory and application of covariance matrix tapers for robust adaptive beamforming," *IEEE Transactions on Signal Processing*, vol. 47, no. 4, pp. 977–985, Apr. 1999.

[5] X. Neyt, F. D. Lapierre, and J. G. Verly, "Estimation of geometric radar configuration parameters for range-dependent compensation in STAP in the presence of targets, jammers and decorrelation effects," in *Proceedings of the IEEE-SAM'04*, Barcelona, Spain, July 2004.